Available online at www.sciencedirect.com
ScienceDirect
Archives of Biochemistry and Biophysics 473 (2008) 48–60
ABB
www.elsevier.com/locate/yabbi

Coupling of folding and DNA-binding in the bZIP domains of Jun–Fos heterodimeric transcription factor

Kenneth L. Seldeen, Caleb B. McDonald, Brian J. Deegan, Amjad Farooq *

Department of Biochemistry & Molecular Biology and the UM/Sylvester Braman Family Breast Cancer Institute, Leonard Miller School of Medicine, University of Miami, 1011 NW 15th Street, Gautier Building, Room 214, Miami, FL 33136, USA

Received 17 January 2008, and in revised form 18 February 2008
Available online 26 February 2008

Abstract

In response to mitogenic stimuli, the heterodimeric transcription factor Jun–Fos binds to the promoters of a diverse array of genes involved in critical cellular responses such as cell growth and proliferation, cell cycle regulation, embryogenic development and cancer. In so doing, Jun–Fos heterodimer regulates gene expression central to physiology and pathology of the cell in a specific and timely manner. Here, using the technique of isothermal titration calorimetry (ITC), we report detailed thermodynamics of the bZIP domains of Jun–Fos heterodimer to synthetic dsDNA oligos containing the TRE and CRE consensus promoter elements. Our data suggest that binding of the bZIP domains to both TRE and CRE is under enthalpic control and accompanied by entropic penalty at physiological temperatures. Although the bZIP domains bind to both TRE and CRE with very similar affinities, the enthalpic contributions to the free energy of binding to CRE are more favorable than TRE, while the entropic penalty to the free energy of binding to TRE is smaller than CRE. Despite such differences in their thermodynamic signatures, enthalpy and entropy of binding of the bZIP domains to both TRE and CRE are highly temperature-dependent and largely compensate each other resulting in negligible effect of temperature on the free energy of binding. From the plot of enthalpy change versus temperature, the magnitude of heat capacity change determined is much larger than that expected from the direct association of bZIP domains with DNA. This observation is interpreted to suggest that the basic regions in the bZIP domains are largely unstructured in the absence of DNA and only become structured upon interaction with DNA in a coupled folding and binding manner. Our new findings are rationalized in the context of 3D structural models of bZIP domains of Jun–Fos heterodimer in complex with dsDNA oligos containing the TRE and CRE consensus sequences. Taken together, our study demonstrates that enthalpy is the major driving force for a key protein–DNA interaction pertinent to cellular signaling and that protein–DNA interactions with similar binding affinities may be accompanied by differential thermodynamic signatures. Our data corroborate the notion that the DNA-induced protein structural changes are a general feature of the bZIP family of transcription factors.

Keywords: Protein–DNA thermodynamics; Isothermal titration calorimetry; Transcription factors Jun and Fos; Basic leucine zipper bZIP; DNA promoter elements TRE and CRE

Protein–DNA interactions play a critical role in coupling extracellular information in the form of growth factors, cytokines, hormones and stress to DNA transcription and, in so doing, regulate a diverse array of cellular processes such as cell growth and proliferation, cell cycle regulation, embryogenic development and cancer. Discovered as components of the transcription factor AP1, Jun and Fos recognize—as Jun–Jun homodimer or Jun–Fos heterodimer—the pseudo-palindromic TGACTCA and palindromic TGACGTCA consensus sequences found in the promoters of a multitude of genes such as metallothionein IIa, collagenase, interleukin 2 and cyclin D1 [1–8]. The consensus sequences TGACTCA and TGACGTCA, respectively, referred to as the TPA (12-*O*-tetradecanoylphorbol-13-ace-

* Corresponding author. Fax: +1 305 243 3955.
E-mail address: amjad@farooqlab.net (A. Farooq).

0003-9861/$ - see front matter © 2008 Elsevier Inc. All rights reserved.
doi:10.1016/j.abb.2008.02.024

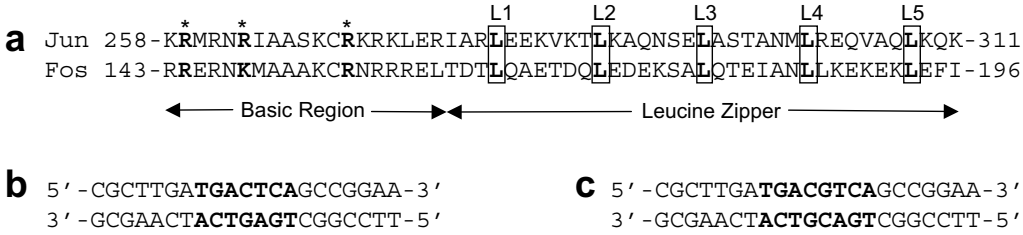

Fig. 1. Protein and DNA sequences. (a) Amino acid sequence alignment of the leucine zipper and basic region in human Jun and Fos that dimerize to form the bZIP domains. The five signature leucines (L1–L5) characteristic of leucine zipper, spaced exactly six residues apart, are boxed and bold faced. The basic residues in the basic region that contact the DNA bases and the backbone phosphates are marked by asterisks and bold faced. (b) Nucleotide sequence of 21-mer dsDNA oligo containing the TRE site (bold faced). (c) Nucleotide sequence of 22-mer dsDNA oligo containing the CRE site (bold faced).

tate) response element (TRE)[1] and the cAMP response element (CRE), occur with a high frequency in the human genome [9,10]. Jun and Fos are expressed in a wide variety of tissues and are subject to activation by a diverse array of mitogenic inputs, including up-regulation by MAP kinases [11,12]. Upon activation, Jun and Fos can switch on gene transcription via their direct involvement and through their co-operation with other transcription factors in the recruitment of the transcriptional machinery to the site of DNA [10,13–16]. Jun and Fos are potent activators of mitogenic transcription and, as such, their hyperactivity is positively correlated with oncogenic transformations of cells [14–16]. To combat such undesirable effects, the activity of Jun and Fos is tightly regulated at various levels, including gene expression, post-translational phosphorylation, and interaction with other cellular proteins [14].

Jun and Fos are modular proteins and contain regions with conserved leucine residues at every seventh position that enable them to form coiled coils termed leucine zippers [7,17]. Located N-terminal to leucine zippers in both proteins are clusters of basic residues that together with leucine zippers constitute what have come to be known as the basic zipper (bZIP) domains of Jun and Fos (Fig. 1a). The bZIP domains enable the recruitment of Jun and Fos to the site of transcription by virtue of their ability to recognize the TRE and CRE consensus sequences in DNA at the promoters of the target genes [7,14]. Once recruited to the site of transcription, Jun and Fos unleash their full transactivation potential and participate in the transcriptional machinery through regions that lie outside the bZIP domains [14,18]. While Jun can homodimerize with itself or heterodimerize with Fos via the formation of leucine zippers to form transcriptionally-active species, the existence of Fos as a homodimer has never been observed under physiological conditions and Fos alone does not possess any transcriptional activity [17].

The availability of 3D structure of the bZIP domains of Jun–Fos heterodimer in complex with dsDNA oligo containing the TRE site has significantly contributed to our understanding of the molecular mechanism of action of this transcription factor at structural level [19]. In this structure, the heterodimeric bZIP domains adopt continuous α-helical conformations of about 15 turns and wrap around each other like a pair of forceps that inserts into the major grooves of DNA via the N-terminal basic regions. While the α-helices are held together by numerous inter-helical hydrophobic contacts and salt bridges, hydrogen bonding between the sidechains of basic residues in the bZIP domains and the sidechains of nucleotides accounts for high affinity binding of bZIP domains to DNA. Further knowledge of how bZIP domains interact with their cognate sequences in DNA comes from kinetic studies that suggest that although bZIP domains of Jun and Fos can heterodimerize rapidly in the absence of DNA, the rate of heterodimerization is significantly enhanced in the presence of DNA and that the pathway in which the bZIP monomers associate with DNA prior to heterodimerization appears to be highly favored on kinetic grounds [20].

Despite such wealth of structural and kinetic data, little is known about the thermodynamic mechanism of the binding of bZIP domains of Fos and Jun to DNA. Here, using the technique of isothermal titration calorimetry (ITC), we report detailed thermodynamics of the bZIP domains of Jun–Fos heterodimer to synthetic dsDNA oligos containing the TRE and CRE consensus promoter elements. Our data suggest that binding of the bZIP domains to both TRE and CRE is under enthalpic control and accompanied by entropic penalty at physiological temperatures. Although the bZIP domains bind to both TRE and CRE with very similar affinities, the enthalpic contributions to the free energy of binding to CRE are more favorable than TRE, while the entropic penalty to the free energy of binding to TRE is smaller than CRE. Despite such differences in their thermodynamic signatures, enthalpy and entropy of binding of the bZIP domains to both TRE and CRE are highly temperature-dependent and largely compensate each other resulting in negligible effect of temperature on the free energy of binding. From the plot of enthalpy change versus temperature, the magni-

[1] *Abbreviations used:* TRE, TPA (12-*O*-tetradecanoylphorbol-13-acetate) response element; CRE, cAMP response element; bZIP, basic zipper; IPTG, isopropyl β-D-1-thiogalactopyranoside; ITC, isothermal titration calorimetry; SEC, size exclusion chromatography; dsDNA, double-stranded DNA; SASA, solvent-accessible surface area.

tude of heat capacity change determined is much larger than that expected from the direct association of bZIP domains with DNA. This observation is interpreted to suggest that the basic regions in the bZIP domains are largely unstructured in the absence of DNA and only become structured upon interaction with DNA in a coupled folding and binding manner. Our new findings are rationalized in the context of 3D structural models of bZIP domains of Jun–Fos heterodimer in complex with dsDNA oligos containing the TRE and CRE consensus sequences. Taken together, our study demonstrates that enthalpy is the major driving force for a key protein–DNA interaction pertinent to cellular signaling and that protein–DNA interactions with similar binding affinities may be accompanied by differential thermodynamic signatures. Our data corroborate the notion that the DNA-induced protein structural changes are a general feature of the bZIP family of transcription factors.

Materials and methods

Protein preparation

bZIP domains of human Jun (residues 251–331) and human Fos (residues 136–216) were cloned into pET102 bacterial expression vector—with an N-terminal thioredoxin (Trx)-tag and a C-terminal polyhistidine (His)-tag—using Invitrogen TOPO technology. Trx-tag was included to maximize protein expression in soluble fraction, while the His-tag was added to aid in protein purification through Ni-NTA affinity chromatography. Additionally, thrombin protease sites were introduced at both the N- and C-termini of the proteins to aid in the removal of tags after purification. Proteins were subsequently expressed in *Escherichia coli* Rosetta2(DE3) bacterial strain (Novagen) cultured in LB media and purified on Ni-NTA affinity column using standard procedures. Briefly, bacterial cells were grown at 20 °C to an optical density of 0.5 at 600 nm prior to induction with 0.5 mM isopropyl β-D-1-thiogalactopyranoside (IPTG). After further overnight growth at 15 °C, the cells were harvested and disrupted using a beadbeater. After separation of cell debris at high speed centrifugation, the cell lysate was subjected to Ni-NTA column and washed extensively with low concentrations of imidazole to remove non-specific binding of bacterial proteins to the column. The recombinant bZIP domains of Jun and Fos were subsequently eluted with 500 mM imidazole and dialyzed against an appropriate buffer to remove imidazole. Further treatment of bZIP domains of Jun and Fos on MonoQ ion-exchange column coupled to GE Akta FPLC system led to purification of recombinant domains to apparent homogeneity as judged by SDS–PAGE analysis. The identity of recombinant proteins was confirmed by MALDI-TOF mass spectrometry analysis. Final yields were typically between 10 and 20 mg protein of apparent homogeneity per liter of bacterial culture. The treatment of recombinant proteins with thrombin protease significantly destabilized the bZIP domains of both Jun and Fos and both domains appeared to be proteolytically unstable. For this reason, all experiments reported herein were carried out on recombinant fusion bZIP domains of Jun and Fos containing a Trx-tag at the N-terminus and a His-tag at the C-terminus. The tags were found to have no effect on the binding of these domains to DNA under all conditions used here. Protein concentrations were determined by the fluorescence-based Quant-It assay (Invitrogen) and spectrophotometrically using extinction co-efficients of 14,230 and 14,230 $M^{-1} cm^{-1}$ at 280 nm for the bZIP recombinant domains of Jun and Fos, respectively. The extinction co-efficients were calculated using the online software ProtParam at ExPasy Server [21]. Results from both methods were in an excellent agreement. Jun–Fos bZIP heterodimers were generated by mixing equimolar amounts of the purified bZIP domains of Jun and Fos. The efficiency of bZIP heterodimerization was close to 100% as judged by Native-PAGE and size exclusion chromatography (SEC) analysis using a Hiload Superdex 200 column.

DNA synthesis

HPLC-grade DNA oligos containing the consensus TRE and CRE sites were commercially obtained from Sigma Genosys. The complete nucleotide sequences of these oligos are presented in Fig. 1b and c. Oligo concentrations were determined spectrophotometrically on the basis of their extinction co-efficients derived from their nucleotide sequences using the online software OligoAnalyzer 3.0 (Integrated DNA Technologies) based on the nearest-neighbor model [22]. To obtain double-stranded DNA (dsDNA) annealed oligos, equimolar amounts of sense and antisense oligos were mixed together and heated at 95 °C for 10 min and then allowed to cool to room temperature. The efficiency of oligo annealing to generate dsDNA was close to 100% as judged by Native-PAGE and size exclusion chromatography (SEC) analysis using a Hiload Superdex 200 column.

ITC measurements

Isothermal titration calorimetry (ITC) experiments were performed on Microcal VP-ITC instrument and data were acquired and processed using fully automized features in Microcal ORIGIN software. All measurements were repeated 2–3 times. Briefly, the protein and DNA samples were prepared in 50 mM Tris, 200 mM NaCl, 5 mM EDTA and 5 mM β-mercaptoethanol at pH 8.0 and de-gassed using the ThermoVac accessory for 10 min. The experiments were initiated by injecting 25 × 10 μl injections of 100–200 μM of dsDNA oligo from the syringe into the calorimetric cell containing 1.8 ml of 5–10 μM of Jun–Fos heterodimer at a fixed temperature in the narrow range 15–35 °C. The bZIP domains of Jun and Fos form heterodimers with an affinity of less than 0.1 μM [20]. Thus, under the ITC conditions, the bZIP domains of Jun and Fos would be expected to predominantly exist as heterodimers with negligible amounts of monomers. The change in thermal power as a function of each injection was automatically recorded using Microcal ORIGIN software and the raw data were further processed to yield binding isotherms of heat release per injection as a function of DNA to protein molar ratio. The heats of mixing and dilution were subtracted from the heat of binding per injection by carrying out a control experiment in which the same buffer in the calorimetric cell was titrated against the dsDNA oligos in an identical manner. Control experiments with scrambled dsDNA oligos generated similar thermal power to that obtained for the buffer alone—as did the titration of dsDNA oligos containing TRE and CRE sites against a protein construct containing thioredoxin with a C-terminal His-tag (Trx–His). Titration of concentrated Trx–His protein construct into the calorimetric cell containing the bZIP domains of Jun–Fos heterodimer produced no observable signal, implying that neither Trx-tag nor His-tag interact with the bZIP domains of Jun and Fos. To extract various thermodynamic parameters, the binding isotherms were iteratively fit to the following in-built function by non-linear least squares regression analysis using the integrated Microcal ORIGIN software:

$$q(i) = (n\Delta HVP/2)\{[1 + (L/nP) + (K_d/nP)] - [[1 + (L/nP) + (K_d/nP)]^2 - (4L/nP)]^{1/2}\} \quad (1)$$

where $q(i)$ is the heat release (kcal/mol) for the ith injection, n is the binding stoichiometry, ΔH is the binding enthalpy (kcal/mol), V is the effective volume of protein solution in the calorimetric cell (1.46 ml), P is the total protein concentration in the calorimetric cell (μM), L is the total concentration of DNA added (μM) and K_d is the apparent equilibrium binding constant (μM). The above equation is derived from the binding of a ligand to a macromolecule using the law of mass action assuming a 1:1 binding stoichiometry [23]. The iterative fit of binding isotherms to the above in-built function thus directly generated values for K_d and ΔH. The free energy change (ΔG) upon ligand binding was calculated from the relationship:

$$\Delta G = RT \ln K_d \quad (2)$$

where R is the universal molar gas constant (1.99 cal/K/mol), T is the absolute temperature in Kelvin and K_d is in the units of mol/L. The entropic contribution ($T\Delta S$) to the free energy of binding was calculated from the relationship:

$$T\Delta S = \Delta H - \Delta G \quad (3)$$

where ΔH and ΔG are as defined above. Heat capacity change (ΔC_p) in the protein upon DNA binding was calculated by measuring ΔH as a function of temperature (T) in the narrow range 15–35 °C—with the slope of the ΔH versus T plot yielding the value of ΔC_p. To improve the accuracy of ITC measurements, the c value was controlled in the approximate range 10–200. The c-value is a dimensionless parameter and defined by the ratio of total protein concentration in the calorimetric cell divided by K_d. Measurements with the c-value outside the range 5–500 are subject to error. Despite the stability conferred upon the bZIP domains of Jun and Fos by the presence of Trx- and His-tags, only the recombinant Jun–Fos heterodimer was stable at protein concentrations above 5 μM needed for ITC experiments, while the recombinant Jun–Jun homodimer lacked the stability for any reliable ITC measurements. For this reason, only ITC measurements on the binding of Jun–Fos heterodimer to DNA are reported in this study.

SASA calculations

The magnitude of changes in polar and apolar solvent-accessible surface area (SASA) in the bZIP domains of Jun–Fos heterodimer upon binding to dsDNA oligos containing the TRE and CRE consensus sites were calculated from thermodynamic data obtained using ITC and compared with those obtained from structural data based on the 3D structural models (see below).

For calculation of changes in polar SASA ($\Delta SASA_{polar}$) and apolar SASA ($\Delta SASA_{apolar}$) upon the binding of dsDNA oligos containing the TRE and CRE consensus sites to bZIP domains of Jun–Fos heterodimer from thermodynamic data, it was assumed that ΔC_p and ΔH at 60 °C (ΔH_{60}) are additive and linearly depend on the change in $\Delta SASA_{polar}$ and $\Delta SASA_{apolar}$ as embodied in the following empirically-derived expressions [24–28]:

$$\Delta C_p = a[\Delta SASA_{polar}] + b[\Delta SASA_{apolar}] \quad (4)$$

$$\Delta H_{60} = c[\Delta SASA_{polar}] + d[\Delta SASA_{apolar}] \quad (5)$$

where a, b, c and d are empirically-determined co-efficients with values of −0.26 cal/mol/K/Å^2, +0.45 cal/mol/K/Å^2, +31.34 cal/mol/Å^2 and −8.44 cal/mol/Å^2, respectively. The co-efficients a and b are independent of temperature, while c and d are referenced against a temperature of 60 °C, which equates to the median melting temperature of the proteins from which these constants are derived [24–26]. ΔC_p was calculated from the slope of a plot of ΔH versus T in the narrow temperature range 15–35 °C for the binding of TRE (−0.87 kcal/mol/K) and CRE (−0.81 kcal/mol/K) dsDNA oligos to the bZIP domains of Jun–Fos heterodimer using the ITC instrument. ΔH_{60} was calculated by the extrapolation of a plot of ΔH versus T to 60 °C for the binding of TRE (−60.56 kcal/mol) and CRE (−64.95 kcal/mol) dsDNA oligos to the bZIP domains of Jun–Fos heterodimer using the ITC instrument. With ΔC_p and ΔH_{60} experimentally determined using ITC and the knowledge of co-efficients a–d from empirical models [24–28], Eqs. (4) and (5) were simultaneously solved to obtain the magnitude of changes in $\Delta SASA_{polar}$ and $\Delta SASA_{apolar}$ independent of structural information upon the binding of dsDNA oligos to the bZIP domains of Jun–Fos heterodimer.

To determine changes in $\Delta SASA_{polar}$ and $\Delta SASA_{apolar}$ upon the binding of dsDNA oligos to bZIP domains of Jun–Fos heterodimer from structural data, two models of binding were assumed—the Rigid Body model and the Induced Fit model. In the Rigid Body model, it was assumed that the bZIP domains of Jun–Fos heterodimer undergo no conformational change upon binding to dsDNA oligos containing TRE and CRE sites. In the Induced Fit model, it was assumed that the basic regions in the bZIP domains of Jun–Fos heterodimer are fully unstructured and only become structured upon binding to dsDNA oligos containing TRE and CRE sites. Changes in $\Delta SASA_{polar}$ and $\Delta SASA_{apolar}$ upon the binding of dsDNA oligos to bZIP domains of Jun–Fos heterodimer from structural data were calculated using the following relationships:

$$\Delta SASA_{polar} = SASA_{bp} - (SASA_{fp} + SASA_{dp}) \quad (6)$$

$$\Delta SASA_{apolar} = SASA_{ba} - (SASA_{fa} + SASA_{da}) \quad (7)$$

where $SASA_{bp}$ and $SASA_{ba}$ are the polar and apolar SASA of bZIP domains of Jun–Fos heterodimer bound to DNA, $SASA_{fp}$ and $SASA_{fa}$ are the polar and apolar SASA of free bZIP domains of Jun–Fos heterodimer, and $SASA_{dp}$ and $SASA_{da}$ are the polar and apolar SASA of free dsDNA oligos. $SASA_{bp}$ and $SASA_{ba}$ were calculated from structural models of bZIP domains of Jun–Fos heterodimer in complex with dsDNA oligos (containing atomic coordinates of both the bZIP domains and the corresponding sense and antisense dsDNA oligos), $SASA_{fp}$ and $SASA_{fa}$ were calculated from structural models of bZIP domains of Jun–Fos heterodimer in complex with dsDNA oligos (but containing atomic coordinates of the bZIP domains only) for the Rigid Body model, while $SASA_{fp}$ and $SASA_{fa}$ were calculated from structural models of bZIP domains of Jun–Fos heterodimer determined in the absence of DNA with basic regions allowed to adopt extended conformations (see below) in the Induced Fit model, and $SASA_{dp}$ and $SASA_{da}$ were calculated from structural models of bZIP domains of Jun–Fos heterodimer in complex with dsDNA oligos (but containing atomic coordinates of only the corresponding sense and antisense dsDNA oligos). All SASA calculations were performed using the online software GETAREA with a probe radius of 1.4 Å [29].

Structural modeling

3D structures of bZIP domains of Jun–Fos heterodimer alone and in complex with dsDNA oligos containing TRE and CRE sites were modeled using the MODELLER software based on homology modeling [30]. The model of bZIP domains of Jun–Fos heterodimer in the absence of DNA was obtained using the crystal structure of bZIP domains of Jun–Fos heterodimer in complex with a dsDNA oligo containing the TRE consensus sequence as a template [PDB code: 1FOS]. However, only the structural coordinates of atoms within leucine zipper regions were used to model the free structure of the bZIP domains of Jun–Fos heterodimer, while the residues in the N-terminal basic regions were allowed to adopt an open extended conformation and allowed to reach the energy minima without any restraints supplied by corresponding residues in the template. The model of bZIP domains of Jun–Fos heterodimer in complex with 21-mer dsDNA oligo containing the TRE site was obtained using the crystal structure of bZIP domains of Jun–Fos heterodimer in complex with a dsDNA oligo containing the TRE consensus sequence TGACTCA but differing in flanking sequences as a template [PDB code: 1FOS]. The model of bZIP domains of Jun–Fos heterodimer in complex with 22-mer dsDNA oligo containing the CRE site was obtained using the crystal structure of bZIP domains of Jun–Jun homodimer in complex with a dsDNA oligo containing the CRE consensus sequence TGACGTCA but differing in flanking sequences as a template [PDB code: 1JNM]. In each case, a total of 100 structural models were calculated and the structure with the lowest energy, as judged by the MODELLER Objective Function, was selected for further energy minimization in MODELLER prior to analysis. The structures were rendered using RIBBONS [31] and superimposed in MOLMOL [32]. All other calculations were performed on the lowest energy-minimized structural model.

Results and discussion

Enthalpy drives the protein–DNA interaction

In an attempt to unravel the thermodynamic mechanism of the binding of bZIP domains of Jun–Fos heterodimer to dsDNA oligos containing the TRE and CRE sites, we

employed the powerful technique of ITC (Fig. 2). Comparison of the various thermodynamic parameters is presented in Table 1. Our data suggest that the bZIP domains of Jun–Fos heterodimer bind to TRE and CRE sites with very similar affinities of 0.15 and 0.21 μM, respectively (Table 1). These observations are in an excellent agreement with previous studies based on semi-quantitative analysis [6,17,33–35]. What sets our study apart from anything previously reported is the striking observation that binding of the bZIP domains of Jun–Fos heterodimer to TRE and CRE sites in DNA is under strong enthalpic control accompanied by entropic penalty at physiological temperatures. This observation is consistent with enthalpic-driven nature of the interaction of the bZIP domains of the yeast transcription factor GCN4 to TRE and CRE sites in DNA [36,37].

The favorable enthalpic change is most likely due to the formation of hydrogen bonding, hydrophobic contacts and electrostatic interactions between the bZIP domains of Jun–Fos heterodimer and its target DNA duplexes as observed in the 3D structure [19]. Interestingly, despite the slightly weaker interaction of the bZIP domains of Jun–Fos heterodimer to CRE site relative to TRE site, the binding to CRE site appears to be enthalpically more favorable by about 5 kcal/mol (Table 1), implying that the presence of an extra base pair between the TGA and TCA half-sites in CRE accounts for favorable electrostatic and hydrophobic interactions with the protein. However, the enthalpic advantage of CRE over TRE is offset by an equally greater entropic penalty, resulting in the overall weaker binding of CRE relative to TRE. This salient observation is in stark contrast to the finding that ΔH is more negative for the binding of bZIP domains of GCN4 to TRE versus CRE [36,37]. However, in these previous studies [36,37], the more favorable ΔH for the binding of bZIP domains of GCN4 to TRE is offset by a much greater entropic penalty relative to CRE and the net result is that, unlike the scenario reported here, it is CRE site that overall appears to bind to GCN4 with a slightly higher affinity relative to TRE site. It is worthy of note that enthalpy-driven nature of protein–DNA interactions observed here is neither a rule nor an exception to the rule, as numerous examples of protein–DNA interactions under enthalpic as well as entropic control have been reported previously [36,38–45].

Although protein–DNA interactions can be driven by either enthalpic or entropic or a combination of both factors [36,39–42,46–48], the large unfavorable entropic change—−75 cal/mol/K for the binding of TRE and −91 cal/mol/K for the binding of CRE—observed here is of significant interest. What might be the molecular basis of such an unfavorable entropy change observed here? Net entropic changes (ΔS) upon protein–DNA interactions are widely considered to result from an interplay between three major entropic forces symbolized as ΔS_{solv}, ΔS_{conf} and ΔS_{mix}. ΔS_{solv} is the favorable entropy change due to

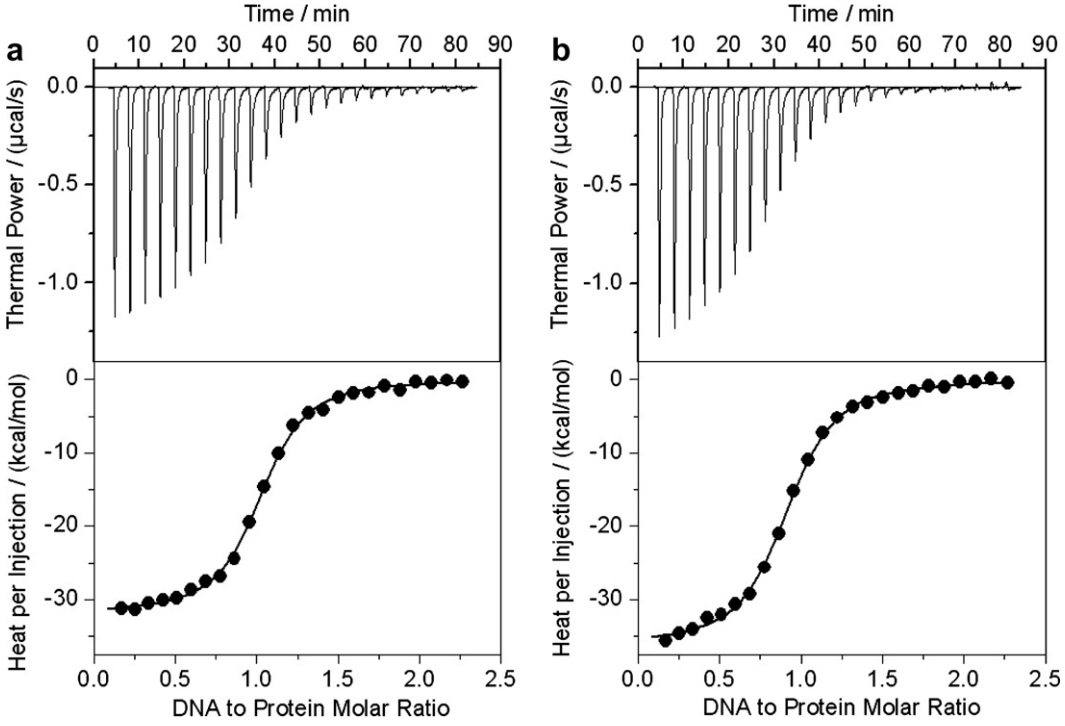

Fig. 2. ITC analysis of the binding of the bZIP domains of Jun–Fos heterodimer to dsDNA oligos containing TRE (a) and CRE (b) sites. bZIP domains of Jun–Fos heterodimer in the calorimetric cell were titrated with 25 × 10 μl injections of dsDNA oligo from the injection syringe at 25 °C. The first injection and the corresponding heat release are not shown due to systematic uncertainties in the measurement. The proteins and the DNA were both in a final buffer of 50 mM Tris, 200 mM NaCl, 5 mM EDTA and 5 mM β-mercaptoethanol at pH 8.0. The solid lines represent the fit of the data to the function based on the binding of a ligand to a macromolecule using the Microcal ORIGIN software [23].

Table 1
Experimentally determined thermodynamic parameters for the binding of bZIP domains of Jun–Fos heterodimer to dsDNA oligos containing TRE and CRE consensus sequences using ITC at 25 °C and pH 8.0

	K_d/μM	ΔH/kcal mol^{-1}	$T\Delta S$/kcal mol^{-1}	ΔG/kcal mol^{-1}
TRE	0.15 ± 0.01	-31.62 ± 0.09	-22.29 ± 0.08	-9.33 ± 0.01
CRE	0.21 ± 0.02	-36.23 ± 0.06	-27.10 ± 0.11	-9.12 ± 0.04

The values for the various parameters shown were obtained from the fit of a function—based on the binding of a ligand to a macromolecule using the law of mass action assuming a 1:1 binding stoichiometry [23]—to the ITC isotherms shown in Fig. 2. The binding stoichiometries to the fits agreed to within ±10%. Errors were calculated from 2–3 independent measurements. All errors are given to one standard deviation.

enhancement in the degrees of freedom of solvent molecules as a result of their restructuring and displacement, particularly around apolar groups, upon molecular associations. In the case of protein–DNA association, the release of counterions from DNA upon binding to protein is also likely to contribute favorably to ΔS_{solv}. ΔS_{conf} is the unfavorable entropic change that arises from the restriction of conformational degrees of freedom of the backbone and sidechain atoms upon molecular associations. It has been suggested that the basic regions in the bZIP domains of Jun–Fos heterodimer are unstructured in the absence of DNA and undergo folding only upon DNA binding [49]. Thus, such restructuring of protein upon DNA binding could further negatively contribute to the ΔS_{conf}. Finally, ΔS_{mix} is the unfavorable entropic change due to the restriction in the translational, rotational and vibrational degrees of freedom of molecules upon binding. Several lines of evidence suggest that ΔS_{mix} typically contributes no more than about −10 cal/mol/K of entropy penalty to the overall entropic change upon binding [27,50–52]. On the basis of these arguments, we attribute the unfavorable entropic change incurred upon the binding of bZIP domains of Jun–Fos heterodimer to DNA largely to the loss of conformational degrees of freedom of backbone and sidechain atoms in both the protein and DNA as embodied in the term ΔS_{conf}.

Enthalpy and entropy compensate the effect of temperature on binding

Thermodynamic behavior of intermolecular associations can be highly dependent on the ambient temperature and knowledge of how thermodynamics vary as a function of temperature can provide invaluable insights into the mechanism of molecular recognition. In an effort to determine the effect of temperature on the various thermodynamic parameters, we analyzed the binding of the bZIP domains of Jun–Fos heterodimer to dsDNA oligos containing the TRE and CRE consensus sites in the temperature range 15–35 °C (Fig. 3). Our data indicate that both the enthalpic (ΔH) and entropic ($T\Delta S$) contributions to the overall free energy of binding (ΔG) show strong temperature-dependence and that both ΔH and $T\Delta S$ largely compensate for

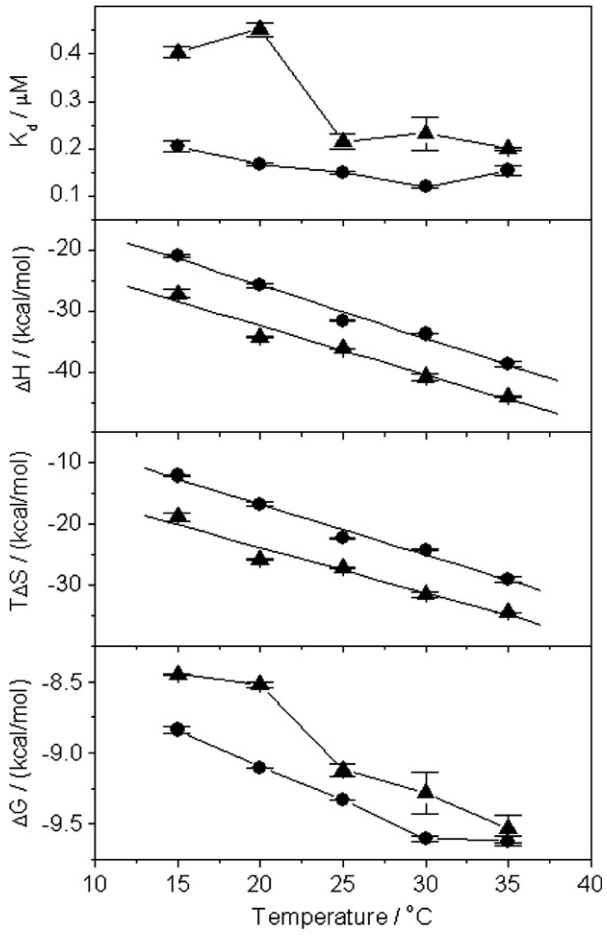

Fig. 3. Dependence of thermodynamic parameters K_d, ΔH, $T\Delta S$ and ΔG on temperature for the binding of bZIP domains of Jun–Fos heterodimer to dsDNA oligos containing TRE (•) and CRE (▲) sites. bZIP domains of Jun–Fos heterodimer in the calorimetric cell were titrated with 25 × 10 μl injections of dsDNA oligo from the injection syringe at various temperatures in the range 15–35 °C. The proteins and the DNA were both in a final buffer of 50 mM Tris, 200 mM NaCl, 5 mM EDTA and 5 mM β-mercaptoethanol at pH 8.0. To determine the various thermodynamic parameters, the ITC isotherms were fit to the function based on the binding of a ligand to a macromolecule using the Microcal ORIGIN software [23]. Each data point is the arithmetic mean of 2–3 experiments. All error bars are given to one standard deviation. The solid lines for the ΔH versus temperature and $T\Delta S$ versus temperature plots show linear fits to the data, while the solid lines for the K_d versus temperature and ΔG versus temperature plots show straight lines merely connecting the data points for clarity.

each other to generate ΔG that is virtually independent of temperature—while ΔH and $T\Delta S$ experience more than 20 kcal/mol change in their contributions to binding in going from 15 to 35 °C, ΔG gains no more than 1 kcal/mol over the same temperature range. Consistent with this observation is the relatively constant nature of the binding affinity (0.1–0.4 μM) over the same temperature range for the interaction of both the TRE and CRE dsDNA oligos with the bZIP domains of Jun–Fos heterodimer. It is of worthy note that the binding affinity for the interaction of bZIP domains with CRE appears to experience a sudden increase from a value of about 0.4 μM at a temperature of

20 °C and lower to a value of about 0.2 μM at a temperature of 25 °C and higher. This unexpected break cannot be accounted for and we do not believe that it is of any significance. We limited our investigations of the effect of temperature on the thermodynamics of protein–DNA interaction within this narrow temperature range due to a number of technical hurdles—below a temperature of 15 °C, the observable ITC signal in the form of thermal power becomes substantially attenuated such that no reliable measurements can be made, while above a temperature of 35 °C, bZIP domains have the tendency to undergo melting and thus measurements at higher temperatures may lead to inconsistencies [36,37]. Regardless of these limitations, our data suggest that within this temperature range, the thermodynamics of binding of the bZIP domains of Jun–Fos heterodimer to TRE and CRE sites are overwhelmingly driven by favorable enthalpic changes with unfavorable entropic contributions to the overall free energy of binding.

The linear and opposing dependence of ΔH and $T\Delta S$ as a function of temperature, while maintaining a more or less constant ΔG, is a common feature observed in protein folding and binding reactions [25,53,54]. This phenomenon implies that there exists a temperature T_H where ΔH contribution to the free energy of binding changes sign. In the case of the binding of bZIP domains of Jun–Fos heterodimer to their DNA duplexes, ΔH will become endothermic and hence thermodynamically unfavorable below this T_H. Our analysis of the dependence of ΔH versus temperature suggests that T_H for the binding of bZIP domains of Jun–Fos heterodimer to TRE and CRE sites is −10 and −20 °C, respectively—the binding of Jun–Fos heterodimer to TRE and CRE sites will be expected to be endothermic below temperatures of about −10 and −20 °C, respectively, and thus under these conditions, entropy not enthalpy is likely to drive the binding process. For further curiosity, we also determined the temperatures at which $T\Delta S$ and ΔG will change sign for the binding of bZIP domains of Jun–Fos heterodimer to TRE and CRE sites in DNA. Extrapolation of the plots of $T\Delta S$ versus temperature suggests that $T\Delta S$ will become positive and hence thermodynamically favorable below temperatures of about 0 and −10 °C for binding to TRE and CRE, respectively. Similarly, extrapolation of the plots of ΔG versus temperature suggests that ΔG will reach zero at approximate temperatures of −210 and −125 °C for binding to TRE and CRE, respectively—the temperatures at which enthalpic and entropic contributions to the free energy of binding will have exactly equal and opposing components.

It is thus striking that despite an entropy penalty encountered at physiological temperatures, the entropy change will be favorable below a temperature of about −10 °C for the binding of Jun–Fos heterodimer to both the TRE and CRE sites in DNA and, below a temperature of about −20 °C, the binding will be predominantly driven by entropic factors with unfavorable contributions from enthalpic forces. We believe that the driving force for binding to switch from being under enthalpic control at physiological temperatures to being under entropic control at lower temperatures is largely due to the change in the ΔS_{conf} component of the overall entropy change of the system. Unlike at physiological temperatures, the change in ΔS_{conf} is unlikely to be the major entropic penalty at lower temperatures due to the loss of reduction in the degrees of freedom of backbone and sidechain atoms available to molecules prior to binding as a result of loss of kinetic energy. Thus, molecular associations may not suffer from the loss of ΔS_{conf} as much as those encountered at higher physiological temperatures. With the ΔS_{conf} penalty being significantly reduced at lower temperatures, the ΔS_{solv} gain as a result of displacement of water molecules surrounding molecular surfaces that become occluded from the solvent upon binding is likely to generate favorable entropic changes needed to drive the binding to completion against the backdrop of unfavorable enthalpic changes—which may also be accounted for by the loss of kinetic energy available for molecular collisions at lower temperatures.

Heat capacity change results from both folding and binding

The temperature-dependence of ΔH is related to heat capacity of binding (ΔC_p) by Kirchhoff's relationship $\Delta C_p = d(\Delta H)/dT$—the slope of a plot of ΔH versus temperature equates to ΔC_p. Heat capacity is an important thermodynamic parameter in that it is related to the extent of the burial, occlusion and dehydration of molecular surfaces from surrounding solvent molecules upon intermolecular association—technically referred to as the change in solvent-accessible surface area (ΔSASA) [25,39,55,56]. As such, this information is critical to understanding the mechanism of molecular recognition and, in the context of protein–DNA interactions, such information can further help us understand the role of thermodynamics pertinent to the regulation of transcriptional machinery.

In an attempt to understand how the binding of Jun–Fos heterodimer to DNA affects SASA, we calculated ΔC_p of −0.87 and −0.81 kcal/mol/K from the slopes of ΔH versus temperature plots obtained for the binding of bZIP domains of Jun–Fos heterodimer to TRE and CRE sites, respectively (Fig. 3). What might be the significance of the negative values of ΔC_p observed here? A positive value of ΔC_p implies that the occlusion of polar surfaces dominates the intermolecular association over apolar surfaces [25,57,58]. The fact that the values of ΔC_p are negative suggests that the occlusion of apolar surfaces dominates the occlusion of polar surfaces for the binding of the bZIP domains of Jun–Fos heterodimer to both the TRE and CRE sites. The slightly more negative ΔC_p for the binding of the bZIP domains of Jun–Fos heterodimer to TRE likely reflects a greater burial of apolar surfaces over polar surfaces for the binding of CRE. Experimental determination of values of ΔC_p combined with ΔH_{60} (enthalpy change at 60 °C) have been widely used to quantitatively calculate changes in polar SASA ($\Delta SASA_{polar}$),

apolar SASA ($\Delta SASA_{apolar}$) and total SASA ($\Delta SASA_{total}$) upon intermolecular association [24–28]. Such changes in SASA upon the binding of bZIP domains of Jun–Fos heterodimer to DNA from our thermodynamic measurements are reported in Table 2.

It has been suggested that the basic regions in bZIP domains are largely unstructured in the absence of DNA and undergo folding only upon binding to DNA [59–63]. Although the solution or crystal structure of the bZIP domains of Jun–Fos heterodimer in the absence of DNA has never been determined, circular dichroism studies provide stern evidence that the basic regions in the bZIP domains of Jun–Fos heterodimer are also unstructured in the absence of DNA and undergo folding only upon DNA binding [49]. In light of this foregoing argument, it is likely that change in SASA determined from our thermodynamic measurements above represents the folding of the basic regions in the bZIP domains of Jun–Fos heterodimer in concert with binding to DNA. To test that this is so, we also determined changes in SASA upon the binding of the bZIP domains of Jun–Fos heterodimer to DNA from structural data independent of our thermodynamic measurements. To calculate changes in SASA upon the binding of the bZIP domains of Jun–Fos heterodimer to DNA from structural data, we assumed two models of binding—the Rigid Body model and the Induced Fit model. In the Rigid Body model, it was assumed that the bZIP domains of Jun–Fos heterodimer undergo no conformational change upon binding to dsDNA oligos containing TRE and CRE sites. In this model, the 3D structure of the bZIP domains of Jun–Fos heterodimer and the dsDNA oligos containing TRE and CRE sites were identical in both the free and the bound states—the Rigid Body model of binding assumes that no folding occurs in the protein or the DNA upon association and that the protein–DNA interaction is solely driven by the binding process alone. In the Induced Fit model, it was assumed that the basic regions in the bZIP domains of Jun–Fos heterodimer are fully unstructured and only become structured upon binding to dsDNA oligos containing TRE and CRE sites—the Induced Fit model of binding assumes that partial folding of the bZIP domains in the basic regions occurs concomitantly upon association and that the protein–DNA interaction is accompanied by both the folding and the binding process.

Table 2 summarizes and compares values for $\Delta SASA_{polar}$, $\Delta SASA_{apolar}$ and $\Delta SASA_{total}$ upon the interaction of the bZIP domains of Jun–Fos heterodimer to TRE and CRE sites, as calculated from our thermodynamic and structural data. Our analysis shows that there are significant deviations between the values calculated from thermodynamic data and the Rigid Body model of binding. In contrast, the values determined from thermodynamic data agree par excellence with those calculated from the Induced Fit model. While the changes in SASA determined from thermodynamic data are off by more than 50% relative to those determined from structural data assuming the Rigid Body model for both TRE and CRE binding, these values agree within about 5% and 20% to those calculated from structural data assuming the Induced Fit model for TRE and CRE binding, respectively. The small anomalies in the values for changes in SASA between those obtained from thermodynamic data versus those calculated from structural data assuming the Induced Fit model are likely due to errors in the atomic coordinates of the structural models. These anomalies particularly become more pronounced in the case of the binding of the bZIP domains of Jun–Fos heterodimer to CRE site due to the poor quality of the 3D structural model of bZIP domains of Jun–Fos heterodimer in complex with CRE versus TRE site. While the structural model of the bZIP domains of Jun–Fos heterodimer in complex with dsDNA oligo containing TRE site was determined from reliable atomic coordinates of the crystal structure of this complex [PDB code: 1FOS], experimental structure of the bZIP domains of Jun–Fos heterodimer in complex with CRE site is not available and thus had to be modeled on the basis of sequence homology with the bZIP domains of Jun–Jun homodimer in complex with CRE site [PDB code: 1JNM].

Table 2
Changes in polar SASA ($\Delta SASA_{polar}$), apolar SASA ($\Delta SASA_{apolar}$) and total SASA ($\Delta SASA_{total}$) upon the binding of bZIP domains of Jun–Fos heterodimer to dsDNA oligos containing TRE and CRE sites

DNA site →	TRE			CRE		
Method →	Thermodynamic	Structural		Thermodynamic	Structural	
Model →	None	Rigid Body	Induced Fit	None	Rigid Body	Induced Fit
$\Delta SASA_{polar}/Å^2$	−2905	−1371	−2602	−3028	−1430	−2507
$\Delta SASA_{apolar}/Å^2$	−3612	−1401	−3489	−3550	−1484	−2499
$\Delta SASA_{total}/Å^2$	−6517	−2772	−6091	−6578	−2914	−5006

The changes in SASA are calculated and compared from both the thermodynamic and structural data. SASA values based on thermodynamic data were obtained from the measurement of ΔC_p for the binding of the bZIP domains of Jun–Fos heterodimer to dsDNA oligos containing TRE and CRE sites (Fig. 3) using expressions (4) and (5), while SASA values based on structural data were derived from 3D structural models of the bZIP domains of Jun–Fos heterodimer alone and in complex with dsDNA oligos containing TRE and CRE sites (Fig. 4) using expressions (6) and (7). For SASA values calculated from structural data, two models were assumed—the Rigid Body model and the Induced Fit model. In the Rigid Body model, it was assumed that the bZIP domains of Jun–Fos heterodimer undergo no conformational change upon binding to DNA. In the Induced Fit model, it was assumed that the basic regions in the bZIP domains of Jun–Fos heterodimer are fully unstructured and only become structured upon binding to DNA. ΔSASA values calculated from thermodynamic data make no assumptions and are thus model-independent.

An alternative explanation for the anomalies observed in the values for changes in SASA between those obtained from thermodynamic data versus those calculated from structural data assuming the Induced Fit model may be due to the assumption that DNA experiences no conformational change upon interaction with the protein in spite of the evidence that it undergoes bending upon binding [64–67]. Nonetheless, this latter assumption is an excellent approximation in our a priori calculations of changes in SASA from structural data due to negligible occlusion of molecular surface in DNA upon bending compared to rather large surface area buried upon protein–DNA contacts coupled with protein folding. It is thus not surprising that, despite small anomalies, our values for changes in SASA upon protein–DNA interaction calculated from thermodynamic data versus those calculated from structural data assuming the Induced Fit model show remarkable consistency. In short, we believe that the significant underestimation of changes in SASA calculated from structural data assuming the Rigid Body model are due to the unrealistic assumption that neither protein nor DNA underwent any conformational change upon the formation of protein–DNA complex. However, in the Induced Fit model of binding, this unrealistic assumption is eliminated. The fact that the changes in SASA obtained from the structural data assuming the Induced Fit model and thermodynamic studies agree to within experimental error unequivocally demonstrates that the bZIP domains of Jun–Fos heterodimer undergo coupled folding and binding to DNA.

Structural modeling allows rationalization of thermodynamic data

In an attempt to rationalize our thermodynamic data in structural terms, we modeled 3D structures of the bZIP domains of Jun–Fos heterodimer alone and in complex with dsDNA oligos containing TRE and CRE sites on the basis of homology modeling (Fig. 4). Given that the insertion of an extra base pair at the center of the CRE site would increase the distance between the TGA and TCA half-sites, our structural models would also test the extent to which the bZIP domains of Jun–Fos heterodimer may have to undergo conformational change to accommodate the wider spacing between these half-sites in the major grooves of DNA.

In agreement with our thermodynamic data, our 3D structural model of the bZIP domains of Jun–Fos heterodimer shows the basic regions unstructured and more or less fully extended in the absence of DNA (Fig. 4a). It is believed that such unfolding occurs due to unfavorable interactions between closely spaced basic residues. However, the basic regions become structured upon the introduction of dsDNA oligos containing TRE and CRE sites due to neutralization of basic charge with negative DNA backbone phosphates (Fig. 4b and c). Our model predicts that the key residues in the basic regions that contact the DNA bases and backbone phosphates would have to undergo significant conformational changes from being fully exposed to solvent to becoming dehydrated upon contact with DNA—a scenario that fully accounts for the magnitudes of ΔC_p observed in our thermodynamic measurements for the binding of bZIP domains of Jun–Fos heterodimer to TRE and CRE sites (Table 2). The conformational changes occurring in the protein upon DNA binding can be best visualized in the form of a movie accessible on the WWW @ http://labs.med.miami.edu/farooq/movies/AP1bZIP.

Consistent with the crystal structure of the protein–DNA complex [19], the bZIP domains of Jun–Fos heterodimer bind to half-sites within the major grooves formed by the TRE site related by a 180° rotation about the dyad axis of the complex (Fig. 4b). One half-site of TRE packs against the basic region of Jun bZIP while the other against the basic region of Fos bZIP. Since the TRE site is pseudo-palindromic, it is believed that the basic regions within Jun and Fos may assume no preferred orientation and that these could easily switch between the two half-sites [19,35]. However, the bZIP domains of Jun–Fos assume asymmetry in that the helical axis of Fos is somewhat straighter than that of Jun and the latter appears to wrap around the straighter axis of Fos. Although the central axis of the coiled-coil bZIP domains of Jun–Fos is almost per-

Fig. 4. Modeled structures of bZIP domains of Jun–Fos heterodimer alone and in complex with dsDNA oligos containing TRE and CRE sites. For clarity, only the core regions of bZIP domains of Jun (residues 258–311) and Fos (residues 143–196) are shown. For the same reason, nucleotides flanking the TRE (TGACTCA) and CRE (TGACGTCA) sites are also omitted. (a) bZIP domains of Jun–Fos heterodimer in the absence of DNA. Leucine zippers are shown in cyan and the basic regions in purple. While the leucine zippers adapt α-helical conformations, the basic regions that contact the DNA are largely unstructured and most likely adapt extended conformations. (b) bZIP domains of Jun–Fos heterodimer in complex with TRE site (yellow). Leucine zippers in the bZIP domains are shown in cyan and the basic regions in purple. The inset shows intermolecular interactions between critical basic residues (green) in bZIP domains and the DNA bases (gray) plus the backbone phosphates (yellow). The structural model was generated using the crystal structure of bZIP domains of Jun–Fos heterodimer in complex with dsDNA oligo containing the TRE site [PDB code: 1FOS] as a template in MODELLER. (c) bZIP domains of Jun–Fos heterodimer in complex with CRE site (yellow). Leucine zippers in the bZIP domains are shown in cyan and the basic regions in purple. The inset shows the intermolecular interactions between critical basic residues (green) in bZIP domains and the DNA bases (gray) plus the backbone phosphates (yellow). The structural model was generated using the crystal structure of bZIP domains of Jun–Jun homodimer in complex with dsDNA oligo containing the CRE site [PDB code: 1JNM] as a template in MODELLER. (d) Superimposition of the orientation of the bZIP domains of Jun–Fos heterodimer in complex with TRE site (red) versus its orientation in complex with CRE site (blue). Superimposition was performed by the alignment of the backbone N, CA and C atoms of the five signature leucines L1, L2, L3, L4 and L5 in each bZIP pair of Jun–Fos heterodimer. The double-headed horizontal arrows compare the distance between the two ends of the bZIP forceps in each of the two complexes in contact with TRE and CRE sites. The double-headed vertical arrow compares the rotation of the bZIP forceps in contact with TRE site relative to CRE site.

pendicular to the double-helical axis of DNA, it is believed that this may not always be the case and that the central axis of the bZIP domains could undergo bending to some degree and that such a flexibility may represent a general feature of the interaction of bZIP domains with DNA [19]. A number of residues in the basic regions of Jun and Fos engage in hydrogen bonding, hydrophobic contacts and electrostatic interactions with the bases and backbone phosphates in the TRE site and are believed to be essential for high affinity binding of Jun–Fos heterodimer to DNA [35,68]. In particular, these include the basic residues R259, R263 and R270 in the basic region of Jun, and R144, K148 and R155 in the basic region of Fos (inset to Fig. 4b).

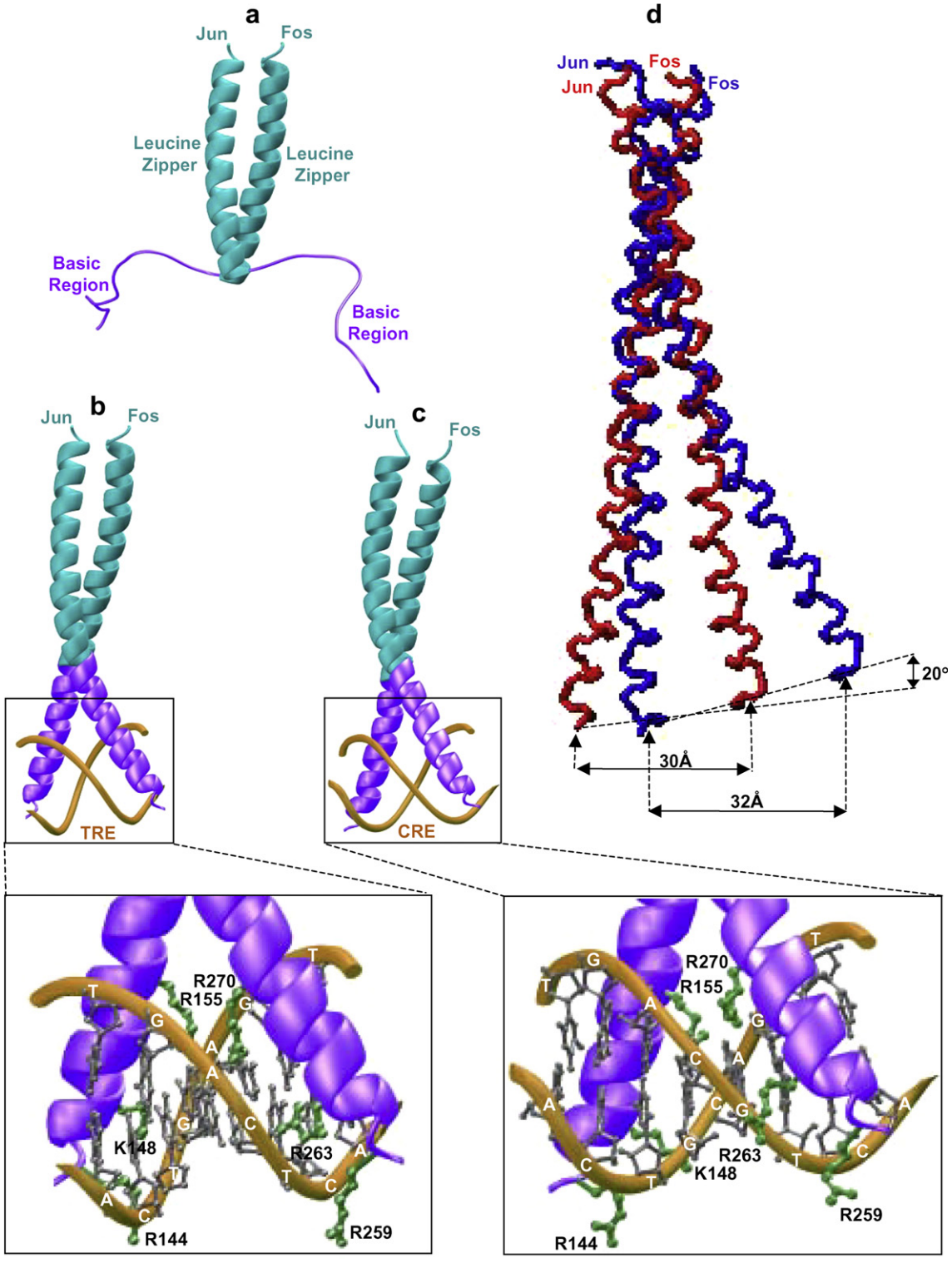

How does an increase in the distance between the TGA and TCA half-sites in the consensus sequence TGACTCA, as a result of insertion of an extra base pair to generate the CRE site, affect the binding of Jun–Fos heterodimer to DNA? As for TRE site, the bZIP domains of Jun–Fos heterodimer bind to CRE site in a very similar manner—the more curved Jun wraps around a straighter Fos and the central axis of the coiled coil Jun–Fos heterodimer is almost perpendicular to the double-helical axis of DNA (Fig. 4c). However, our structural model of the bZIP domains of Jun–Fos in complex with CRE site suggests that the increase in the distance between the TGA and TCA half-sites would be compensated by a slight re-orientation of the basic regions in the bZIP domains of Jun–Fos heterodimer so as to splay apart the bZIP forceps and re-align the key residues in the basic regions that contact the DNA bases and backbone phosphates (inset to Fig. 4c). Additionally, the extra G insert at the center of the CRE site would contribute to strong favorable hydrogen bonding and hydrophobic interactions with the bZIP domains of Jun–Fos heterodimer. These additional protein–DNA interactions may also account for the more favorable enthalpic change observed upon the binding of bZIP domains of Jun–Fos heterodimer to CRE site relative to TRE site (Table 1).

Superimposition of bZIP domains of Jun–Fos heterodimer in complex with TRE site versus CRE site reveals that the backbone atoms of basic regions in Jun and Fos open up by about 2 Å at their N-termini in contact with major grooves of DNA (Fig. 4d). This increase in the distance is consistent with the knowledge that the addition of an extra base pair to DNA adds about 3 Å to its double-helical length. Furthermore, there is also a rotation of about 20° of the bZIP domains of Jun–Fos heterodimer in complex with CRE site relative to TRE site due to the insertion of an extra base pair. Binding of bZIP domains of Jun–Fos heterodimer to CRE site is further aided by the slight bending of DNA relative to that in TRE site. Our model of bZIP domains of Jun–Fos heterodimer in complex with CRE site also predicts that the residues in the basic regions of both Jun and Fos that are critical for interaction with TRE site are also likely to play a key role for interaction with CRE site and that the insertion of an extra base pair does not alter the pattern of protein–DNA interactions. These observations are in an excellent agreement with the crystal structure of the bZIP domains of GCN4 in complex with CRE site [69,70].

Apart from the subtle differences in the protein and DNA conformations mentioned above, both the TRE and CRE sites appear to occlude similar surface areas at the protein–DNA interface upon binding (Table 2). Although the larger CRE site would be expected to engage in more extensive contacts with DNA and hence lead to greater occlusion of surface area upon binding, the conformational change in the protein necessary to accommodate the larger CRE site appears to counterbalance this due to slight re-arrangement of residues at the protein–DNA interface. Nonetheless, the additional contacts made by the introduction of an extra base pair between the TGA and TCA half-sites manifests itself in the form of additional release of heat of about 5 kcal/mol relative to TRE site upon binding to the bZIP domains of Jun–Fos heterodimer. This favorable gain in enthalpy is, however, offset by an equal but opposing amount of unfavorable entropic cost for the binding of CRE site relative to TRE site, making the latter site equally favorable, if not more favorable, for binding the Jun–Fos heterodimer.

Conclusions

Although critical role of the Jun–Fos heterodimeric transcription factor in cellular signaling was reported over two decades ago [1–8], thermodynamics of this key protein–DNA interaction have hitherto not been reported. Knowledge of thermodynamics is central to understanding the intrinsic forces that determine the structure and stability of protein–DNA interactions. In an attempt to elucidate the role of various thermodynamic forces at play in the binding of the Jun–Fos heterodimer to DNA, we have reported herein a detailed ITC analysis of this key protein–DNA interaction pertinent to cellular signaling and cancer. The lack of availability of such thermodynamic information over the past two decades underlies the difficulties of biophysical analysis of free bZIP domains and this has been particularly problematic in the case of the bZIP domains of Jun–Fos heterodimer. However, the knowledge that tagging recombinant proteins with thioredoxin may enhance their stability in solution led to our success with being able to work with recombinant thioredoxin-tagged bZIP domains of Jun–Fos heterodimer under conditions necessary for their biophysical analysis and thus gaining invaluable insights into the thermodynamics of this key protein–DNA interaction.

One might be tempted to question the validity of our thermodynamic data due to the enhanced stability afforded by the presence of thioredoxin tag at the N-termini of bZIP domains of Jun and Fos. However, we have shown herein that the thioredoxin tag does not physically interact with either bZIP domain and that its role here is simply to enhance the bZIP stability through its ability to offset the balance of destabilizing interactions of bZIP domains with water molecules. In this regard, the thioredoxin tag may act as a blessing-in-disguise in that it may impart upon bZIP domain a conformation more reminiscent to that found in the context of full-length Jun or Fos protein. On the contrary, thermodynamic studies on untagged isolated bZIP domains could also raise the question of their validity as these domains may behave in a slightly differential manner when taken out of the context of a full-length protein. Ideally, one would like to carry out studies of this nature on bZIP domains in the context of their full-length proteins but given that their expression and purification could pose new challenges, one will always be reduced to work with some sort of assumptions.

Given the reasonable assumption that the thioredoxin tag is unlikely to alter the thermodynamic properties of bZIP domains in any significant way, our study shows for the first time that the binding of Jun–Fos heterodimer to DNA is under enthalpic control and that this process is accompanied by an unfavorable loss of entropy at physiological temperatures. We attribute this entropic penalty to the loss of conformational degrees of freedom of backbone and sidechain atoms in both the protein and DNA upon binding. The net entropic change (ΔS) can be decomposed into the following major entropic contributions:

$$\Delta S = \Delta S_{solv} + \Delta S_{conf} + \Delta S_{mix}$$

where ΔS_{solv}, ΔS_{conf} and ΔS_{mix} are the entropic contributions due to restructuring of solvent, changes in conformational degrees of freedom of backbone and sidechain atoms, and changes in translational, rotational and vibrational degrees of freedom upon binding, respectively. While ΔS_{solv} has been shown to be equal to $\Delta C_p \ln[T/385]$ (where T is the absolute temperature), ΔS_{mix} is essentially the cratic entropy for a bimolecular reaction and equates to -8 cal/mol/K [27,51]. From the experimentally determined values of ΔC_p here (Fig. 3), ΔS_{solv} for the binding of bZIP domains of Jun–Fos heterodimer to TRE and CRE can be shown to be equal to +226 and +210 cal/mol/K, respectively, at 25 °C. Thus, given that ΔS for the binding of bZIP domains of Jun–Fos heterodimer to TRE and CRE is, respectively, -75 and -91 cal/mol/K at 25 °C (Table 1), ΔS_{conf} for the binding of bZIP domains of Jun–Fos heterodimer to both TRE and CRE turns out to be -293 cal/mol/K at 25 °C. In other words, the entropic penalty due to the loss of conformational degrees of freedom of backbone and sidechain atoms in both the protein and DNA upon binding is -293 cal/mol/K at 25 °C. However, this penalty is largely compensated by the favorable entropic gain of +226 and +210 cal/mol/K at 25 °C due to the restructuring and displacement of water molecules upon the binding of bZIP domain of Jun–Fos heterodimer to TRE and CRE sites, respectively.

Although it has been known that the bZIP domains of Jun–Fos heterodimer could recognize both the TRE and CRE sites [6,34,35], our study here shows that the binding of Jun–Fos heterodimer to both sites occurs with almost indistinguishable affinities and that differences in the thermodynamic parameters ΔH and $T\Delta S$ largely compensate for each other without any significant impact on the overall ΔG for binding. This is remarkably striking given that the insertion of an extra base pair between the TGA and TCA half-sites is expected to increase the distance between them by about 3 Å. Our structural models of bZIP domains of Jun–Fos heterodimer in complex with TRE and CRE sites suggest that this increase in distance between the TGA and TCA half-sites is counteracted by an equally accommodating conformational change in the protein that allows the basic regions in the bZIP domains to open up by about 2 Å at the protein–DNA interface and further undergo a rotation of about 20° relative to their positions in contact with TRE site in DNA. The magnitude of heat capacity changes and associated changes in SASA upon protein–DNA interaction determined from ITC measurements suggest strongly that the basic regions in the bZIP domains of Jun–Fos heterodimer are partially unstructured and become structured only upon interaction with DNA in a coupled folding and binding manner. This finding corroborates the notion that the coupled folding and DNA-binding is a general feature of the bZIP family of transcription factors [59–63].

Finally, current strategies for the design of drugs that can inhibit the oncogenic action of Jun–Fos heterodimer on cellular machinery are based on molecules that either interfere with the heterodimerization, or alternatively, compete with TRE and CRE sites for binding to Jun–Fos heterodimer. Our demonstration that the Jun–Fos heterodimer undergoes conformational change upon DNA binding may offer novel opportunities for the design of drugs that lock the Jun–Fos heterodimer in its partially unstructured state so as to completely abrogate its DNA binding potential.

Acknowledgments

This work was funded by grants from the UM/Sylvester Braman Family Breast Cancer Institute and the American Heart Association to AF (Grant # 0655087B).

References

[1] W. Lee, A. Haslinger, M. Karin, R. Tjian, Nature 325 (1987) 368–372.
[2] D. Bohmann, T.J. Bos, A. Admon, T. Nishimura, P.K. Vogt, R. Tjian, Science 238 (1987) 1386–1392.
[3] W. Lee, P. Mitchell, R. Tjian, Cell 49 (1987) 741–752.
[4] P. Angel, E.A. Allegretto, S.T. Okino, K. Hattori, W.J. Boyle, T. Hunter, M. Karin, Nature 332 (1988) 166–171.
[5] B.R. Franza Jr., F.J. Rauscher 3rd, S.F. Josephs, T. Curran, Science 239 (1988) 1150–1153.
[6] F.J. Rauscher 3rd, P.J. Voulalas, B.R. Franza Jr., T. Curran, Genes Dev. 2 (1988) 1687–1699.
[7] T. Curran, B.R. Franza Jr., Cell 55 (1988) 395–397.
[8] F.J. Rauscher 3rd, D.R. Cohen, T. Curran, T.J. Bos, P.K. Vogt, D. Bohmann, R. Tjian, B.R. Franza Jr., Science 240 (1988) 1010–1016.
[9] H. Zhou, T. Zarubin, Z. Ji, Z. Min, W. Zhu, J.S. Downey, S. Lin, J. Han, DNA Res. 12 (2005) 139–150.
[10] Y. Chinenov, T.K. Kerppola, Oncogene 20 (2001) 2438–2452.
[11] A.J. Whitmarsh, R.J. Davis, J. Mol. Med. 74 (1996) 589–607.
[12] R. Pramanik, X. Qi, S. Borowicz, D. Choubey, R.M. Schultz, J. Han, G. Chen, J. Biol. Chem. 278 (2003) 4831–4839.
[13] A.D. Baxevanis, C.R. Vinson, Curr. Opin. Genet. Dev. 3 (1993) 278–285.
[14] P. Angel, M. Karin, Biochim. Biophys. Acta 1072 (1991) 129–157.
[15] G. Raivich, A. Behrens, Prog. Neurobiol. 78 (2006) 347–363.
[16] K. Milde-Langosch, Eur. J. Cancer 41 (2005) 2449–2461.
[17] T.D. Halazonetis, K. Georgopoulos, M.E. Greenberg, P. Leder, Cell 55 (1988) 917–924.
[18] R. Alani, P. Brown, B. Binetruy, H. Dosaka, R.K. Rosenberg, P. Angel, M. Karin, M.J. Birrer, Mol. Cell Biol. 11 (1991) 6286–6295.
[19] J.N. Glover, S.C. Harrison, Nature 373 (1995) 257–261.
[20] J.J. Kohler, A. Schepartz, Biochemistry 40 (2001) 130–142.

[21] E. Gasteiger, C. Hoogland, A. Gattiker, S. Duvaud, M.R. Wilkins, R.D. Appel, A. Bairoch, Protein identification and analysis tools on the ExPASy server, in: J.M. Walker (Ed.), The Proteomics Protocols Handbook, Humana Press, 2005, pp. 571–607.
[22] C.R. Cantor, M.M. Warshaw, H. Shapiro, Biopolymers 9 (1970) 1059–1077.
[23] T. Wiseman, S. Williston, J.F. Brandts, L.N. Lin, Anal. Biochem. 179 (1989) 131–137.
[24] S.P. Edgcomb, K.P. Murphy, Curr. Opin. Biotechnol. 11 (2000) 62–66.
[25] K.P. Murphy, E. Freire, Adv. Protein Chem. 43 (1992) 313–361.
[26] D. Xie, E. Freire, Proteins 19 (1994) 291–301.
[27] K.P. Murphy, Med. Res. Rev. 19 (1999) 333–339.
[28] E. Freire, Arch. Biochem. Biophys. 303 (1993) 181–184.
[29] R. Fraczkiewicz, W. Braun, J. Comp. Chem. 19 (1998) 319–333.
[30] M.A. Marti-Renom, A.C. Stuart, A. Fiser, R. Sanchez, F. Melo, A. Sali, Annu. Rev. Biophys. Biomol. Struct. 29 (2000) 291–325.
[31] M. Carson, J. Appl. Crystallogr. 24 (1991) 958–961.
[32] R. Koradi, M. Billeter, K. Wuthrich, J. Mol. Graph 14 (51–55) (1996) 29–32.
[33] H. Kwon, S. Park, S. Lee, D.K. Lee, C.H. Yang, Eur. J. Biochem. 268 (2001) 565–572.
[34] R.P. Ryseck, R. Bravo, Oncogene 6 (1991) 533–542.
[35] Y. Nakabeppu, D. Nathans, Embo J. 8 (1989) 3833–3841.
[36] C. Berger, I. Jelesarov, H.R. Bosshard, Biochemistry 35 (1996) 14984–14991.
[37] A.I. Dragan, L. Frank, Y. Liu, E.N. Makeyeva, C. Crane-Robinson, P.L. Privalov, J. Mol. Biol. 343 (2004) 865–878.
[38] J.H. Ha, R.S. Spolar, M.T. Record Jr., J. Mol. Biol. 209 (1989) 801–816.
[39] J.E. Ladbury, J.G. Wright, J.M. Sturtevant, P.B. Sigler, J. Mol. Biol. 238 (1994) 669–681.
[40] D. Foguel, J.L. Silva, Proc. Natl. Acad. Sci. USA 91 (1994) 8244–8247.
[41] V. Petri, M. Hsieh, M. Brenowitz, Biochemistry 34 (1995) 9977–9984.
[42] E. Merabet, G.K. Ackers, Biochemistry 34 (1995) 8554–8563.
[43] M. Sieber, R.K. Allemann, Nucleic Acids Res. 28 (2000) 2122–2127.
[44] K. Datta, V.J. LiCata, Nucleic Acids Res. 31 (2003) 5590–5597.
[45] K. Datta, A.J. Wowor, A.J. Richard, V.J. LiCata, Biophys. J. 90 (2006) 1739–1751.
[46] X. Wang, W. Cao, A. Cao, L. Lai, Biophys. J. 84 (2003) 1867–1875.
[47] S. Milev, H.R. Bosshard, I. Jelesarov, Biochemistry 44 (2005) 285–293.
[48] S. Milev, A.A. Gorfe, A. Karshikoff, R.T. Clubb, H.R. Bosshard, I. Jelesarov, Biochemistry 42 (2003) 3481–3491.
[49] L. Patel, C. Abate, T. Curran, Nature 347 (1990) 572–575.
[50] X. Siebert, L.M. Amzel, Proteins 54 (2004) 104–115.
[51] K.P. Murphy, D. Xie, K.S. Thompson, L.M. Amzel, E. Freire, Proteins 18 (1994) 63–67.
[52] A. Tamura, P.L. Privalov, J. Mol. Biol. 273 (1997) 1048–1060.
[53] K.P. Murphy, V. Bhakuni, D. Xie, E. Freire, J. Mol. Biol. 227 (1992) 293–306.
[54] R.S. Spolar, M.T. Record Jr., Science 263 (1994) 777–784.
[55] P.L. Privalov, S.J. Gill, Adv. Protein Chem. 39 (1988) 191–234.
[56] R.S. Spolar, J.H. Ha, M.T. Record Jr., Proc. Natl. Acad. Sci. USA 86 (1989) 8382–8385.
[57] P.L. Privalov, G.I. Makhatadze, J. Mol. Biol. 224 (1992) 715–723.
[58] R.S. Spolar, J.R. Livingstone, M.T. Record Jr., Biochemistry 31 (1992) 3947–3955.
[59] M.A. Weiss, T. Ellenberger, C.R. Wobbe, J.P. Lee, S.C. Harrison, K. Struhl, Nature 347 (1990) 575–578.
[60] M.A. Weiss, Biochemistry 29 (1990) 8020–8024.
[61] H.R. Bosshard, E. Durr, T. Hitz, I. Jelesarov, Biochemistry 40 (2001) 3544–3552.
[62] V. Saudek, A. Pastore, M.A. Castiglione Morelli, R. Frank, H. Gausepohl, T. Gibson, F. Weih, P. Roesch, Protein Eng. 4 (1990) 3–10.
[63] K.S. Thompson, C.R. Vinson, E. Freire, Biochemistry 32 (1993) 5491–5496.
[64] D.A. Leonard, N. Rajaram, T.K. Kerppola, Proc. Natl. Acad. Sci. USA 94 (1997) 4913–4918.
[65] R.J. Diebold, N. Rajaram, D.A. Leonard, T.K. Kerppola, Proc. Natl. Acad. Sci. USA 95 (1998) 7915–7920.
[66] D.A. Leonard, T.K. Kerppola, Nat. Struct. Biol. 5 (1998) 877–881.
[67] M. John, R. Leppik, S.J. Busch, M. Granger-Schnarr, M. Schnarr, Nucleic Acids Res. 24 (1996) 4487–4494.
[68] L.J. Ransone, J. Visvader, P. Wamsley, I.M. Verma, Proc. Natl. Acad. Sci. USA 87 (1990) 3806–3810.
[69] J. Kim, K. Struhl, Nucleic Acids Res. 23 (1995) 2531–2537.
[70] P. Konig, T.J. Richmond, J. Mol. Biol. 233 (1993) 139–154.